A STUDY OF MICROSTRUCTURE AND FATIGUE BEHAVIOUR OF A3003 ALLOY

[1]Jan ŠKODA, [1]Monika LOSERTOVÁ, [1]Kateřina KONEČNÁ, [2]František FOJTÍK, [3] Petr CZYŽ

[1]VSB - Technical University of Ostrava, Faculty of Materials Science and Technology, Ostrava, Czech Republic, EU, *jan.skoda@vsb.cz*
[2]VSB - Technical University of Ostrava, Faculty of Mechanical Engineering, Ostrava, Czech Republic, EU,
[3]Hanon Systems Autopal s.r.o., NovýJičín, Czech Republic, EU

Abstract

A study of A3003 aluminium alloy in H12 temper regarding microstructure analysis, tensile testing, fatigue loading and fractography of fracture surfaces was carried out. Specimens were cyclic loaded at five stress amplitude levels of 62, 68, 70, 72 and 76 MPa so that the results for both the low cycle fatigue and high cycle fatigue are obtained. During loading of the specimens at the highest stress amplitude the specimens resembled quasi-static fracture with necking usually seen in tensile testing. In our case, the stress amplitude of 72 MPa can be considered transient as the failure went from quasi-static fracture to fracture with typical signs of fatigue. The 68 MPa stress amplitude appears as a transition from LCF to HCF. Testing at the lowest stress amplitude was stopped after 10^7 cycles without failure of the material so it can be regarded as fatigue limit for this alloy. Wrought microstructure was observed using optical microscopy and present phases were identified by EDX analysis as Al_6FeMn and $\alpha\text{-}Al_{12}(Fe,Mn)_3Si$. The microstructure of H12 temper was compared with the same alloy in F state.

Keywords: Low cycle fatigue, high cycle fatigue, A3003, fracture, Al-Mn

1.   INTRODUCTION

Al-Mn based aluminium alloys are widely used throughout the industry. They are not suitable for highly stressed components as their main advantages are good formability, excellent corrosion resistance and specific strength rather than ultimate strength. In automotive industry, these alloys are mostly used for components in air conditioning as pipelines, condensers, containers, heat shields etc. With growing demand on performance of automobiles, the request for cooling also grows. Switching form internal combustion engines to electrical engines does not decrease the needs for effective cooling of the components and aluminium alloys are considered very effective solution with good cost, low weight and good possibilities for recycling but also with a lot of space for further research regarding their mechanical properties and especially fatigue properties. This study was focused on fatigue behaviour of the A3003-H12 alloy and fracture surfaces evaluation with regard to the number of loading cycles. The microstructure of the specimens was compared with the same alloy in F temper. Unlike H12 temper that describes work hardened to quarter hard and not annealed stage, F temper is "semi-finished" (otherwise as fabricated) stage with no property limits specified.

2.   METHODOLOGY & EXPERIMENTAL

The investigation included microstructure analysis, phase analysis, tensile testing, fatigue testing and fractographic study of the fracture surfaces after loading with aim to evaluate fatigue behaviour of the alloy in H12 temper, to compare the fracture surfaces after low cycle fatigue (LCF) and high cycle fatigue (HCF). The alloy in rod shaped specimens was supplied by Hanon Systems Autopal s.r.o. company. In total 5 polished specimens of 60 mm overall length, with 30 mm working length and 5 mm working diameter were prepared for

the tensile testing and 14 polished specimens with 100 mm overall length, 50 mm working length and 6 mm working diameter for fatigue testing. Fatigue loading was carried out using servo-hydraulic single axis pulsator INOVA FU-63-930-V1 equipped with PC with TestControl_FU63 software. Tests were performed in load control mode using symmetric cycle at 5 levels of stress amplitude – 62, 68, 70, 72 and 76 MPa to obtain results for both low cycle fatigue (LCF) and high cycle fatigue (HCF) [1]. The study of fracture surfaces after tensile testing and after cyclic loading was performed using JEOL JSM-649OLV scanning electron microscope (SEM) equipped with OXFORD INSTRUMENTS INCA x-act tool for EDX microanalysis. Microstructure analysis was carried out on selected specimens using Olympus GX51 optical microscope (OM) with DP1 digital camera. Grain shape and size were showed after electrolytic colour etching in a solution composed of 5 ml 48 % HBF_4 and 200 ml H_2O using Struers Lectropol–5 device.

3.   RESULTS AND DISCUSSION

Selected specimens were subjected to the microstructure and phase analysis using both OM and SEM. When comparing the longitudinal cuts of the tested specimens, small phases elongated and oriented in the forming direction can be seen for both H12 and F tempers (**Figure 1a** and **Figure 1c**). The cross sections of the specimens show similar results with phases and grains having in most cases approximately equiaxed shape (**Figures 1b** and **1d**).
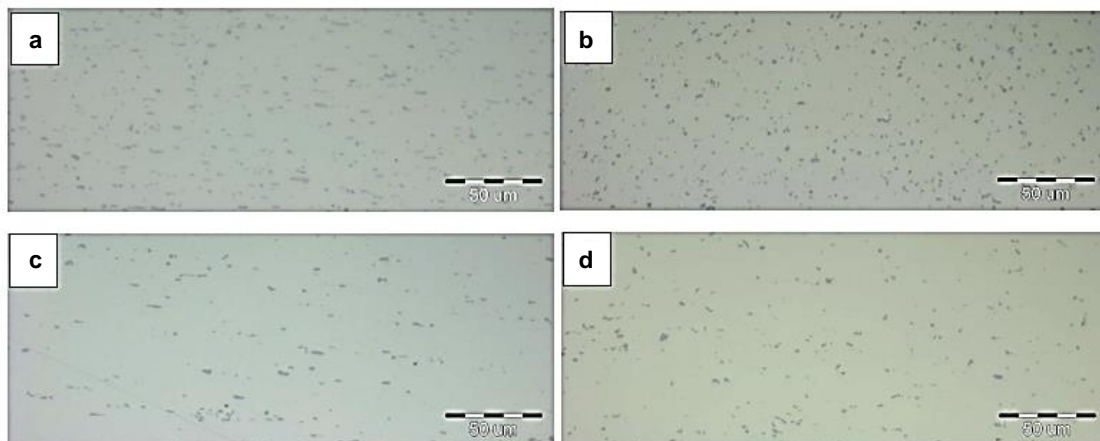

Figure 1 Microstructure of the specimens: a) longitudinal section of H12 temper, b) cross section of H12 temper, c) longitudinal section of F temper, d) cross section of F temper

The F temper contains fine particles of the similar size to that in H12 temper, but their distribution seems to be denser for the H12 temper. The phases observed were analysed using EDX analysis which confirmed the presence of α-$Al_{12}(Fe,Mn)_3Si$ and $Al_6(Fe,Mn)$ particles. The distribution of the phases can be controlled by alloy composition and heat treatment so called "6 to alpha" transformation [2, 3], which supports growth of the α-$Al_{12}(Fe,Mn)_3Si$ phase with higher strength, while the $Al_6(Fe,Mn)$ particles dissolve. Complete dissolution of the phases mentioned is very complicated due to danger of melting at higher annealing temperatures [4]. Both phases can affect recrystallisation and precipitation processes and through of this fatigue resistance of the alloy. Finding detailed information about the effects of the phases mentioned above on fatigue behaviour of the alloy is very difficult. When looking at OM images of colour etched samples, it can be clearly seen that the grains have been elongated in the direction of forming as mentioned before (**Figures 2a, 3a**). The F temper shows much more profound deformation of the grains, which can be attributed to the fact, that recrystallisation annealing was not applied and the grains remained in deformed state (**Figures 3a, 3b**). We can also observe differences in size of the grains in the H12 temper (**Figure 2b**). The difference can be caused by thermo-mechanical history of the H12 temper and possible dynamic recrystallisation processes occurring during extrusion [5].
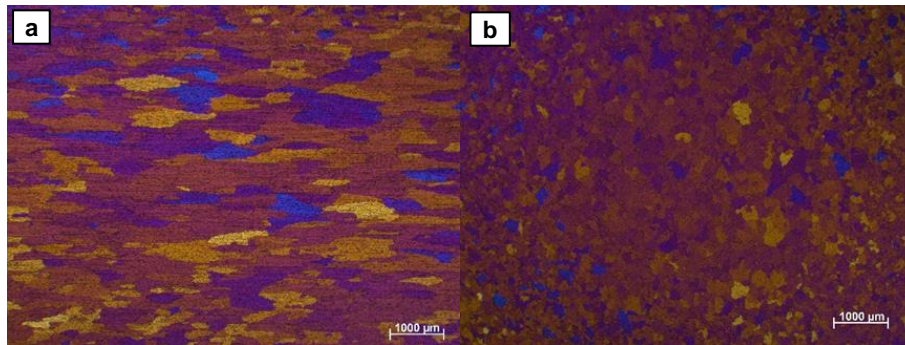
Figure 2 Colour etched microstructure of H12 temper: a) longitudinal, b) cross section
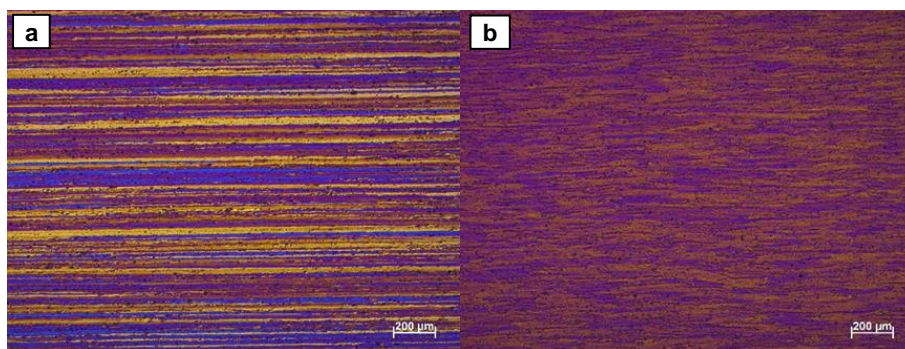

Figure 3 Colour etched microstructure of F temper: a) longitudinal, b) cross section

The yield strength $R_{p0,2}$ and ultimate tensile strength R_m obtained by tensile testing (**Table 1**) are within the specifications of the A3003 alloy [6] with approximate yield strength of 117 MPa and ultimate tensile strength of 123 MPa. Low difference between $R_{p0,2}$ and R_m corresponds with the H12 temper industrial data sheets.

Table 1 Results of tensile testing for A3003-H12 samples

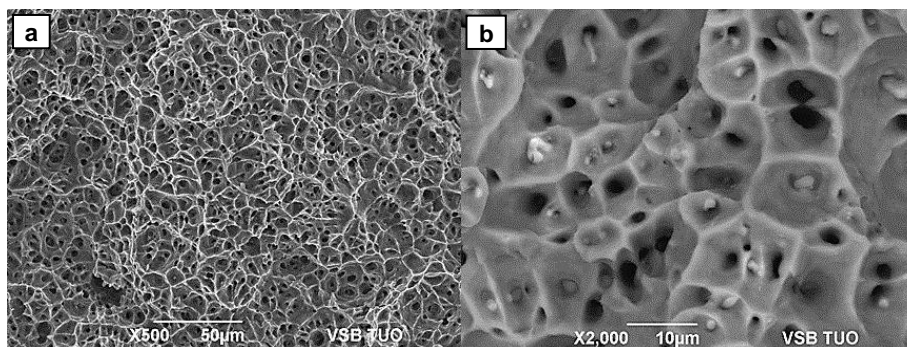| Sample	$R_{p0.2}$ (MPa)	R_m (MPa)
1	116	123
2	117	123
3	121	124
4	118	123
5	117	123
Average value	118 ± 1.9	123 ± 0.4

Figure 4 SEM image of fracture surface for the specimen 1 after tensile testing: a) surface with ductile dimples, b) detail of remaining phases observed in SEM BEI mode

During the tensile testing, all specimens have been deformed with typical necking in the area of final rupture. As it can be seen in **Figure 4a**, fracture surface shows signs of ductile character with dimples and no visible grain boundaries which points out to ductile transgranular fracture. The image performed in backscattered electrons mode (SEM BEI) shows remaining phases inside the dimples which probably acted as initiation sites for the failure (**Figure 4b**).

Fatigue testing has been carried out using load control mode and symmetrical cycle of loading at five stress amplitudes with 20 Hz testing frequency. Used stress amplitudes were chosen in correlation with [1] to cover both LCF and HCF. Results of the tensile testing can be seen in **Table 2**.

Table 2 Results of fatigue testing for A3003-H12 samples

Specimen No.	σ_a(MPa)	Cycles executed	Result
2	76	9,991	Fractured with necking
3	76	9,245	Fractured with necking
4	76	7,551	Fractured with necking
10	72	14,915	Fractured with necking
11	72	38,813	Fractured
12	72	36,563	Fractured
13	70	39,211	Fractured
14	70	77,193	Fractured
1	68	2,754,924	Fractured
5	68	210,231	Fractured
6	68	1,265,631	Fractured
7	62	10,069,149	Unbroken
8	62	10,169,378	Unbroken
9	62	10,135,993	Unbroken

In the column of cycles executed some fluctuation of the results is evident. The widest range of values was obtained for the 68 MPa stress amplitude. The most probable cause is some defect in the surface layer, which significantly reduced the time (number of cycles needed) for microcracks propagation for the sample 5 or 6. Specimens tested at the highest stress amplitude (76 MPa) have been fractured with presence of necking similar to the tensile testing, without typical signs of fatigue on the fracture surfaces (**Figure 5**). The deformation of these samples reminds cyclic creep (ratcheting) even without the presence of nominal stress for which the ratcheting is typical [7].
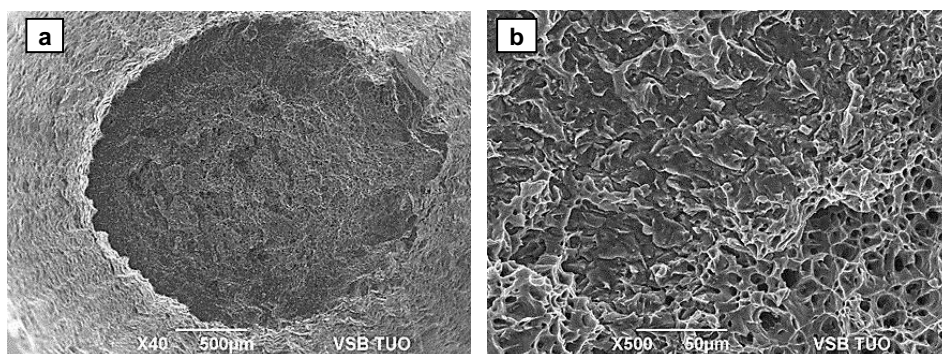

Figure 5 SEM fractography for the specimen 2 after fatigue loading at 76 MPa: a) general view of the fracture surface, b) detail of the surface with two different mechanisms of crack propagation

The stress amplitude level of 72 MPa could be considered transitional as two results were obtained: one type of fracture was similar to the ones obtained at the highest stress level amplitude and the second type was typical fatigue fracture with radial steps, beachmarks, striations and final overload fracture (**Figure 6**).
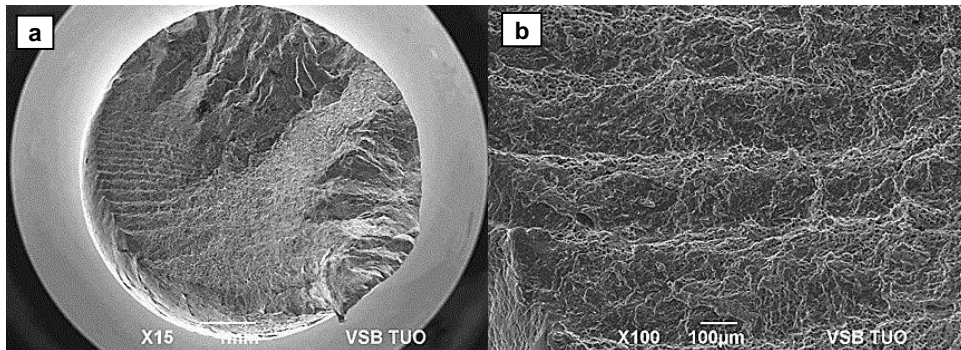

Figure 6 SEM fractography for the specimen 11 after fatigue loading at 72 MPa (LCF): a) general view of the fracture surface, b) detail of alternating crack propagation mechanisms

In this case, the 68 MPa stress amplitude level could be considered as a transition from LCF to HCF with the number of cycles in magnitude of 10^5 to 10^6. Even though there is massive difference in the number of cycles, the fracture surfaces look very similar (**Figure 7**). This is in accordance with the theory behind the big difference in the number of cycles executed. While more than 90% of lifetime of the material during fatigue loading is consumed by microcracks propagation, the process of fatigue crack propagation after the initiation is relatively fast [8].
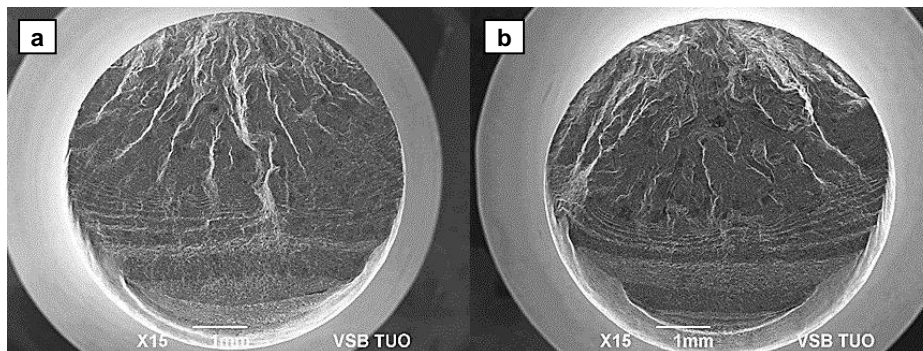

Figure 7 SEM fractography for the specimens after fatigue loading at 68 MPa: a) specimen 1 (after 10^6 cycles), b) specimen 5 (after 10^5 cycles)

Important difference in fracture feature of the specimens loaded at 72 MPa or 68 MPa consists in ratio of ductile and brittle fields. Indeed, for the specimen loaded at higher stress amplitude the area of faster crack propagation with alternating mechanism of ductile/brittle crack propagation occupies bigger part of the surface and the individual marks are bigger and further away from each other. Testing on the lowest stress amplitude was ended after 10^7 cycles without failure of the specimens, therefore in these conditions the stress amplitude of 62 MPa can be considered as the fatigue limit for this alloy [9].Microhardness evaluation showed a trend of slight increasing hardness with increasing amount of deformation accumulated in the material. Nevertheless, the differences in microhardness are relatively small with average HV0.1 values of 48 and 43 for H12 and F tempers, respectively.

4. CONCLUSION

The study of the mechanical properties and microstructure was carried out for A3003-H12 alloy. The alloy was subjected to tensile and fatigue testing. During the tensile testing, specimens have been deformed with the presence of typical necking in the area of fracture. Values of the tensile strength obtained correspond with specifications of the alloy. During the fatigue loading (LCF) at 72 MPa stress amplitude two results were obtained: first with deformation and necking of the specimen similar to the tensile testing and with no marks of fatigue on the fracture surface, second with typical fatigue fracture features. Lower stress amplitudes resulted in typical fatigue failures with initiation sites, radial steps, beachmarks, striations and final overload fractures. The main difference between the LCF and HCF fracture surfaces observed consisted in different proportions of the areas with different mechanisms of crack propagation. The lowest stress amplitude of 62 MPa can be considered as fatigue limit of the alloy under these conditions as there was no damage observed even after 10^7 numbers of cycles. Furthermore, the microstructure and microhardness of H12 and F tempers of the same alloy composition were compared. Microhardness values measured for both states showed increasing trend relating with thermo-mechanical treatment applied during material processing when F temper proved lowest hardness.

REFERENCES

[1]   YAGUCHI, H. Fatigue-damage evaluation in aluminum heat-transfer tubes by measuring cell-wall thickness. *Materials Science and Engineering.* 2001, vol. 315, pp. 189-194.

[2]   DU, Quiang. Microstructural modeling of the homogenization heat treatment for AA3XXX alloys. *JOM.* [online]. 2011, vol. 63, issue 7, pp. 35-39. Available from: https://doi.org/10.1007/s11837-011-0107-1.

[3]   ALEXANDER, D.T.L. Solid-state intermetallic phase transformations in 3XXX aluminium alloys. *Acta Materialia.* 2002, vol. 50, pp. 2571-2583.

[4]   ŠKODA, J. Study of fatigue fractures of Al-Mn alloy. In: *IOP Conf. Ser.: Mater. Sci. Eng.* Prague, 2019, pp. 461-467.

[5]   MAHMOODKHANI, Y. The development of grain structure during axisymmetric extrusion of AA3003 aluminum alloys. *Metallurgical and Materials Transactions.* 2015, vol. 46, issue 12, pp. 5920-5932.

[6]   Atlas steels. *Aluminium Alloy Data Sheet 3003.* [online]. 2015, 1, 2 [viewed: 2021-05-07]. Available from: www.atlassteels.com.au

[7]   SURAJIT, K.P. A critical review of experimental aspects in ratcheting fatigue: microstructure to specimen component. *Journal of Materials Research and Technology.* 2019, vol. 8, issue 5, pp. 4894-4914.

[8]   MILELLA, Pietro Paolo. *Fatigue and Corrosion in Metals.* London: Springer, 2013.

[9]   ASM 05224G. *Elements of Metallurgy and Engineering Alloys.* Materials Park, Ohio, USA: ASM International, 2008.